

Phosphonate additives do not always inhibit crystallization

Andrew Baynton*, Brett D. Chandler[^], Franca Jones^{‡*}, Gareth Nealon*, Mark I. Ogden*, Tomoko Radomirovic*, George K. H. Shimizu[^], Jared M. Taylor[^]

Received (in XXX, XXX) Xth XXXXXXXXXX 200X, Accepted Xth XXXXXXXXXX 200X

5 First published on the web Xth XXXXXXXXXX 200X

DOI: 10.1039/b000000x

This paper investigates crystal growth modifiers based on 1,3,5-substituted benzene derivatives. The results show that as expected, the phosphonated derivative inhibits calcite precipitation to a much greater degree than the analogous sulfonate. However, on barium sulfate, both molecules
10 show some crystallization promotion behaviour, with the phosphonate being the more potent promoter overall. Thus, the functional group alone does not determine the impact the organic molecule will have on crystallization. This opens the way for additives that have dual purposes (inhibiting the crystallization of one phase while not impacting or promoting the crystallization of other phases).

15

Introduction

Scale is essentially any unwanted crystallization that occurs in a process. Barium sulfate is a well known scale compound usually encountered during the production of oil from off-
20 shore rigs.¹⁻³ It is also a relatively simple precipitation system that is sometimes used as a model system.⁴ Calcite can also be found as a scale in some processes^{5, 6} but is more interesting due to its abundant presence as a biomineral.⁷⁻⁹ There is a vast amount of previous literature describing the effect of various
25 organics on the precipitation of barium sulfate and calcium carbonate (for example¹⁰⁻¹⁷). Additives can dramatically affect particle shape and size and therefore can be used in a particle engineering sense, i.e. to obtain the desired physical properties of the particles in question.¹⁸ Additives can also
30 inhibit nucleation and growth and be used as scale inhibitors¹⁹, or they may even increase the rate of crystallization and be used as promoters.^{20, 21} Despite this activity, there are still many fundamental questions to be answered in terms of the mechanism(s) by which additives
35 interact with the crystallization process.

Previous work in this field has sought to understand inhibition in terms of the so called lattice-matching criteria and the functional groups present. Recently however, it has
40 been shown that functional groups that were believed not to impact on barite crystallization can have an effect²²⁻²⁴ and that lattice matching does not always predict strength of inhibition.²³

In this paper, we are expanding on previous work looking at rigid molecules²³ in order to further investigate the
45 structure activity relationships determining the efficacy of crystal growth modifiers. We chose to fix the backbone structure (benzene ring) and modify the functional group, being either a sulfonate or phosphonate moiety. Both these functionalities are well known to inhibit barite and calcite
50 crystallization. Moreover, previous work would suggest that the sulfonate group will be less potent than the phosphonate group in its inhibitory action.^{21, 14}

Experimental

The materials used in this study were AR grade, from Ajax
55 Chemicals or BDH and were dissolved to the required concentrations using ultrapure (>18 MΩcm resistivity) water. Filtered water (0.2 μm), having a resistivity of ≥18 MΩcm⁻¹, was used throughout. Organic additives were synthesized in-house according to literature procedures.^{25, 26} Schematic
60 diagrams of these molecules are shown in Figure 1.

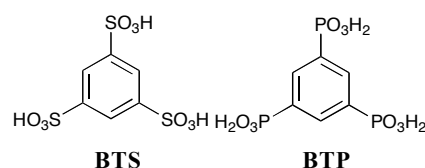


Figure 1. Organic additives investigated in this work: BTS = benzene-
65 1,3,5-trisulfonate BTP = benzene-1,3,5-triphosphonate

Conductivity

Unseeded, de-supersaturation curves were obtained using a reactor vessel kept at 25°C by a water bath and monitored
70 using conductivity (WTW LF 197 Conductivity meter). An overhead stirrer (150 rpm) was used to keep the solids in suspension. The method of barite precipitation consisted of equilibrating 0.249 mM BaCl₂ and adding 1 mol equivalent of Na₂SO₄ solution to initiate crystallization as described in a
75 previous publication.²¹ The total volume for all experiments was 201 mL. The graph of conductivity versus time was used to calculate k (de-supersaturation rate) by fitting the linear region of the de-supersaturation curve. The pH for all experiments was 6.0 except where specified. Organic
80 additives were added to the barium chloride solution prior to the addition of sulfate. The de-supersaturation rate was found to have an error of ~10%.

The supersaturation S can be defined, such that $S=c/c_0$

(where c is the concentration of the ion and c_0 is the equilibrium solubility concentration). This was adopted since no data on the association between BTP or BTS and barium or calcium ions is available. When the ions forming the crystallizing salt are present at 1:1 ratios and the activity of the ions is ~ 1 , this approximation is reasonable. The barium BTS salt was found to be reasonably soluble while the barium BTP salt was sparingly soluble at best. Thus, we can exclude salt formation for the barium-BTS system. In addition, we calculated the expected conductivity values for the barium-BTP system and could exclude salt formation for this situation also. The observed rates were also normalized to the control, i.e. k/k_0 where k_0 is the de-supersaturation rate (in the linear region of the curve) for the control run (absence of impurity) and k is the de-supersaturation rate for the experiment with impurity present. A value of 1 implies it is similar to the control, less than 1 implies inhibition and >1 implies crystallization promotion.

Light Scattering measurements

Absorbance was measured using a UV-Vis instrument (GCB) operated at 900 nm wavelength using a quartz flow cell. When absorbance by the solution and solids is low, this is equivalent to measuring the turbidity (or light scattered) of a system.²⁷ The induction time is defined as the time prior to the turbidity exceeding background levels²⁸ and is related to the nucleation rate for that system.²⁸ For the barite precipitation experiments, the barium chloride concentration, sodium sulfate concentrations and temperature were all equivalent to those used in the conductivity experiments. The flow rate through the cell was 67 mL/min and this was achieved using a Masterflex® peristaltic pump and Tygon® tubing.

Calcium Carbonate Crystal Growth

Calcium carbonate crystals were grown slowly in the presence of additives, by diffusion of carbon dioxide and ammonia into a calcium chloride solution, as described previously.¹⁹ Four open beakers containing calcium chloride solutions (10 mL, 7 mmol) and the appropriate concentrations of the additives were placed in a glass dish (14 cm diameter, 7 cm deep). In order to facilitate the recovery of the crystals, microscope coverslips (pre-soaked in 1M HCl and rinsed with ultrapure water and dried) were placed in the beakers. Four open vials of water (ca. 15 mL) were placed adjacent to the beakers, and a vial of solid ammonium carbonate (ca. 1g) with a plastic screw cap punctured by a single needle hole was placed in the middle of the other containers. The glass dish was then sealed. The coverslips were recovered after 4 days, rinsed with water and dried in air before being sputter coated with gold prior to viewing under the SEM. Additive solutions were added as pH 6 adjusted solutions.

In addition, seeded growth experiments were conducted using the pH stat method.²⁹ Briefly; a 6.2 mM solution of Ca^{2+} and HCO_3^{2-} was prepared by the addition of CaCl_2 solution (0.05 M, 8 mL) and NaHCO_3 solution (0.1 M, 4 mL) to a

solution of NaCl and KCl (0.1 M and 0.011 M respectively, 50 mL). A concentrated aqueous stock solution of the additive was added, and the volume made up to 65 mL by the addition of ultrapure water to give the desired final concentration. The pH of the solution was adjusted to 8.80 by the addition of KOH solution (0.05 M). Crystallisation was initiated by the addition of solid CaCO_3 (5.0 mg) and the pH maintained at 8.80 by the controlled addition of KOH solution (0.05 M) using a pH-stat titration program on an automatic titrator (Mettler DL67 Titrator, Mettler Toledo DG 111-SC pH probe). The volume of KOH solution added to maintain the pH as a function of time was recorded. The mixture was vigorously agitated at all times by an overhead stirrer. The BTP was prepared as an acid solution and added directly since pH stat measurement adjusts pH to 8.8.

Scanning electron microscopy (SEM)

For the barium sulfate runs, samples were collected by filtration onto 0.20 μm membranes. After washing and drying in a desiccator, a portion of the filter paper was placed onto carbon coated stubs and stored in a desiccator. The samples were gold sputtered prior to viewing in a Philips XL30 or Zeiss Evo SEM. Calcium carbonate crystals were crystallized on washed and dried glass cover slips. The cover slips were collected from the crystallization vials, washed and dried and placed on a carbon coated SEM stub. Carbon paint was applied to the edges of the glass cover slip to minimize charging effects.

Atomic Force Microscopy (AFM)

AFM experiments were performed on a PicoPlus using a standard silicon nitride cantilever with a flow through cell attachment. The same procedure was used for all samples. A freshly cleaved barium sulfate mineralogical sample was fixed to a metallic stub and the flow cell was flushed with filtered (Gelman 0.2 μm Supor® membrane filters) ultrapure water (resistivity $>18 \text{ M}\Omega\text{cm}$) using a precision dual syringe pump run at 0.2 mL/min. One syringe then had the water replaced with barium chloride solution (0.1 mM) and the other with sodium sulfate solution (0.1 mM). This was then flushed through the cell at a rate of 0.2 mL/min as per the water. Finally, the barium chloride solution was replaced with a solution containing barium chloride plus the additive of interest at a known concentration and the sodium sulfate solution was topped up as necessary. This was then flushed through the cell at a rate of 0.2 mL/min as per the water and pure barium sulfate run. In this way, the rate of growth of the original barium sulfate could be measured and the difference to when impurity was added could be gauged.

Results and Discussion

Morphology of barium sulfate

The effect of the two organic molecules on the precipitation of barium sulfate is best summarized by the images shown in

Figure 2.

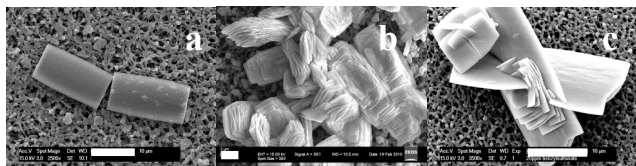


Figure 2. a) control (barium sulfate only). Barium sulfate formed in the presence of b) 26 μM BTP and c) 52 μM BTS (size bars are 10 μm for A and C and 2 μm for B)

Experiments were also undertaken at a low supersaturation in order to determine the effect of the various impurities more precisely. Figure 3 shows the impact of adding BTP to the crystallization of barium sulfate at $S=7$. It can be seen that the particles become much more twinned (as seen at the higher supersaturations) and that the c axis is lengthened with respect to the control (double headed arrow in 3a and b) suggesting an increased relative rate of growth in the c direction. This c axis lengthening can be either due to inhibition of the other faces or promotion of the c axis. At higher concentrations of BTP, rounding at the (001) face ends of the particles is observed (Figure 3c), which suggests that inhibition of the barium sulfate crystallization is occurring.

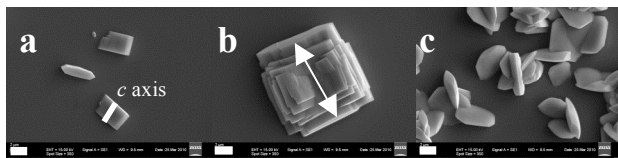


Figure 3. SEM images of barium sulfate particles formed at $S=7$ and a) 0 b) 0.001 mM c) 0.01 mM BTP (all size bars = 2 μm)

When BTS is added there is also a notable c axis lengthening (Figure 4b-c) though not to the same degree. In addition, at high concentrations of BTS, there is indication that the barium sulfate particles are being inhibited as was found for BTP and also that there is substantial twinning occurring.

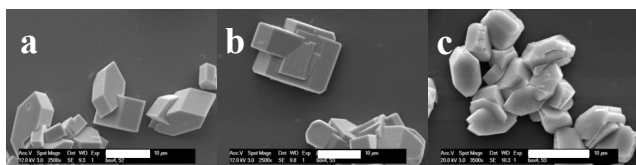


Figure 4. SEM images of barium sulfate particles obtained at $S=5$ and in the presence of a) 0 mM b) 0.02 mM, c) 0.04 mM BTS (circle shows magnified area in inset, all size bars = 10 μm)

De-supersaturation rate of barium sulfate

The conductivity curves (Figure 5) did not always show a significant impact on de-supersaturation. In fact, for BTS there is no difference in de-supersaturation rate (error is

$\pm 10\%$) while for the BTP there is significant crystallization promotion peaking at $\sim 13 \mu\text{M}$.

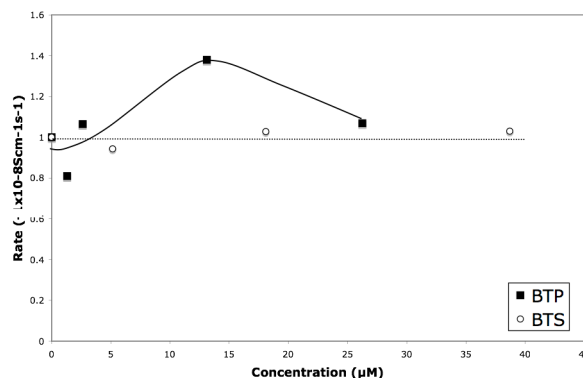


Figure 5. Normalised de-supersaturation rates of barium sulfate versus concentration of BTP (closed squares) or BTS (open circles) present (lines drawn to aid reader only)

Given that twinning of the barite crystals is observed both in the presence of BTS and BTP it is somewhat surprising that the presence of BTS does not show any effect on de-supersaturation rate. There are two possible explanations for this; i) the BTS inhibits surface nucleation events while still enhancing growth thus canceling out the effect of each, or ii) the two molecules impact on different barite faces in different ways while the conductivity only gives the average effect on all of the barite faces. Hence, light scattering and AFM were undertaken to better determine the mechanisms by which the sulfonate and phosphonate molecules are interacting with the crystal surface.

Light Scattering/Turbidity

The light scattering results showed that the BTS initially increased the induction time at low additive concentrations but the impact did not change significantly as the additive concentration was increased (Figure 6a). Thus, BTS inhibits bulk nucleation slightly. This in turn means that BTS is altering the critical nuclei surface free energy and thereby also altering the critical nucleus size.²⁸ This suggests, as mentioned above, that the BTS could actually promote crystal growth but by inhibiting nucleation, the overall de-supersaturation rate remains unaltered. The BTP shows a weaker effect whereby the induction time of barium sulfate is still seen to increase but to a lesser degree (Figure 6b).

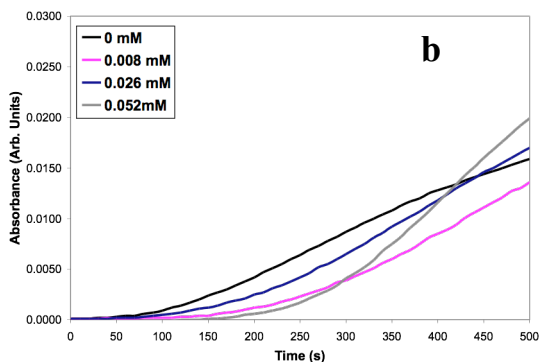
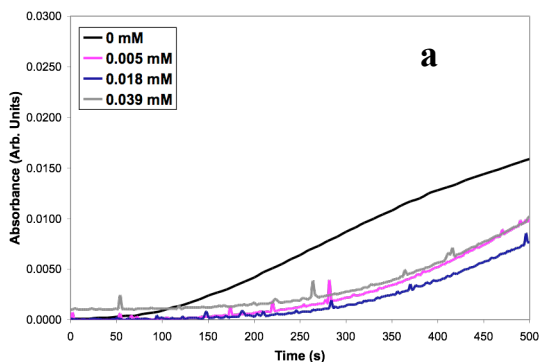


Figure 6. Turbidity curves for barium sulfate precipitation in the presence of varying a) BTS and b) BTP concentration

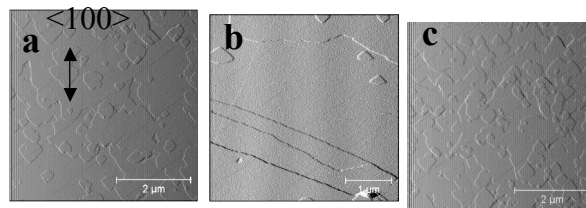


Figure 7. 5x5 μ m AFM in-situ deflection images of the (001) growth at S=5 in the presence of a) 0mM impurity (control) b) 0.02 mM BTS and c) 0.009 mM BTP

Neither BTS nor BTP altered the growth island shape, confirming that at these concentrations step pinning was not occurring. BTS shows a lowering of the number of surface nuclei but the growth rate shows an increase in the $\langle 100 \rangle$ direction, at least for low concentrations (Figure 8). As the concentration of BTS increases, the rate of growth in the $\langle 100 \rangle$ direction decreases to similar values to the control. The presence of BTP does not change the rate of growth compared to the control if the large errors are taken into consideration. The results presented here support the turbidity results in that nucleation of barium sulfate is inhibited by the presence of BTS (both 3D and 2D nucleation) but BTS appears to promote the growth of the (001) barium sulfate face at low concentrations, which also correlates well with the low S morphology results. Thus, in the case of BTS growth is promoted but nucleation is inhibited.

AFM

The AFM of barium sulfate growth on the (001) face in the presence and absence of these inhibitors confirms some of the mechanistic information already obtained. Figure 7 shows some snapshot images during the *in situ* growth of the (001) face of barium sulfate in the presence of the organics. Since the $\langle 100 \rangle$ is the slowest growing direction of the growth sector, this direction was chosen to reflect the impact of the impurities on the growth rate and is shown by the double headed arrow in Figure 7a. The number of new surface nuclei observed in each scan was also measured to determine the effect on surface nucleation events. Since the supersaturation is below the homogenous nucleation S value ($S > 7-10$) we can assume that all new growth islands are due to 2D nucleation on the (001) surface. It must be stressed that because nucleation is a stochastic process, 20 such observations per concentration were recorded and only the average is presented.

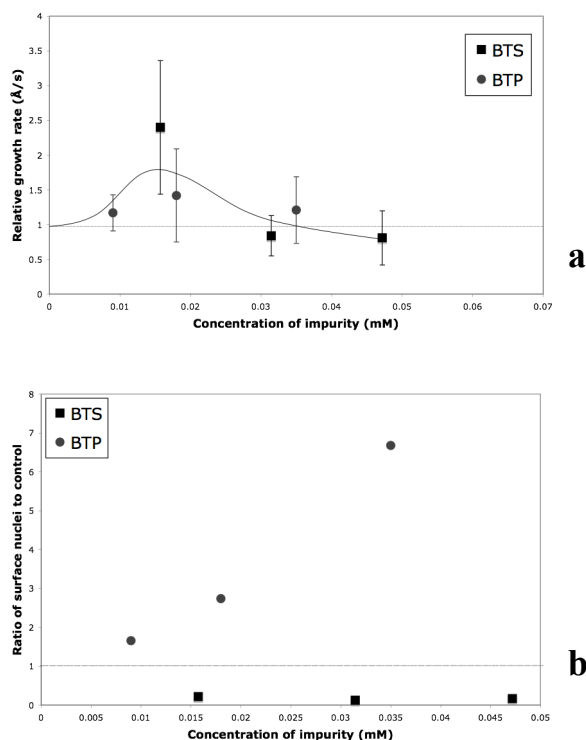


Figure 8. a) Growth rate in the $\langle 100 \rangle$ direction relative to the control and b) the average number of new surface nuclei on a $5 \times 5 \mu\text{m}$ area per scan period (259sec) relative to the control

The BTP on the other hand promotes surface nucleation on the (001) face while little impact is observed on the growth rate.

Calcium carbonate morphology

The effects of BTS and BTP on calcium carbonate crystallization were also investigated. Figure 9 shows the effect on morphology. The control picture shows well-defined calcite rhombs present (Fig.9a). The BTS has a significant impact on calcite morphology provided the concentration is high enough (Fig.9c versus Fig.9d). Here the calcite particles are 'cowbell' shaped; almost rhombic at one end and significantly amorphous looking at the other. The BTP, however, already has a significant effect on calcite morphology at $26 \mu\text{M}$ concentrations. For calcium carbonate then, both molecules appear to be inhibitors and the BTP appears to be a much stronger inhibitor than the BTS. This confirms the typical phosphonate versus sulfonate inhibitory trend observed previously.^{21, 14}

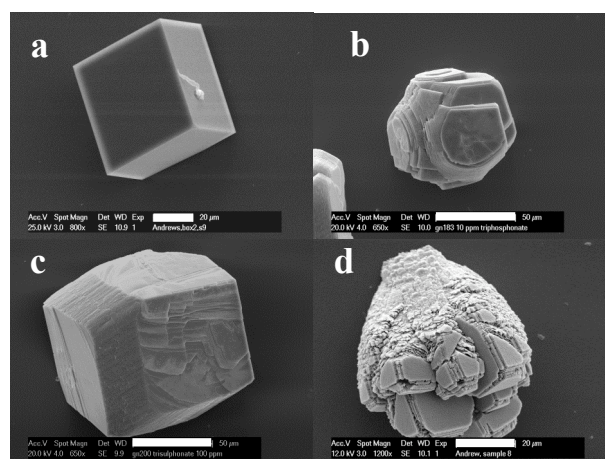


Figure 9. The effect of the sulfonated impurities on calcium carbonate crystallization a) 0 mM impurities b) 0.026 mM BTP c) 0.26 mM and d) 1.3 mM BTS (size bars are $20 \mu\text{m}$ in a & d and $50 \mu\text{m}$ in b & c)

Calcium carbonate growth

The results above were supported by the pH stat growth experiments that showed that both BTS and BTP inhibited the growth of calcite seeds. Once again, the BTP was observed to be more potent as an inhibitor than the BTS. At the lower concentrations, the concentration of BTP required to give approximately the same inhibition as BTS is ~ 150 times less. However, as concentration increases, this reduces to ~ 6 .

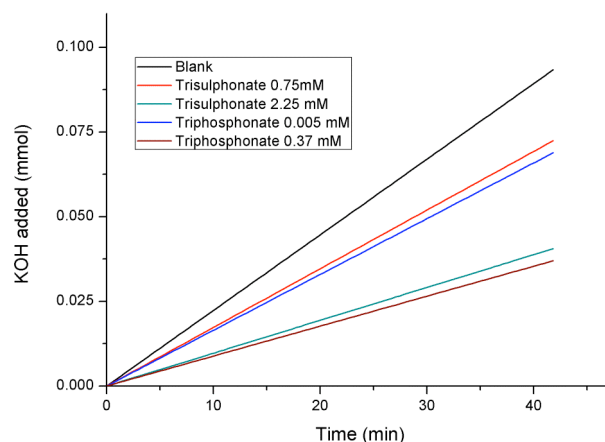


Figure 10. pH stat results for calcium carbonate seed particles grown in the absence and presence of BTS and BTP

Inhibitor or promoter?

The impact of these molecules on calcium carbonate is relatively straightforward – they are inhibitors with the phosphonate derivative being a more potent inhibitor than the sulfonate. This is as one would expect from previous work.^{19, 14} The unusual aspect of this work has been the differences observed in behaviour of the two molecules on the different inorganic species. For barium sulfate, despite the BTS and BTP molecules having functional groups at 'lattice matching'

positions²³ there is very little inhibition. On the (001) face BTS is able to promote barium sulfate crystallization at very low concentrations and supersaturations but the main impact appears to be on nucleation, 2D and 3D (AFM and nephelometry results). Remarkably, the impact of BTP on barium sulfate is essentially to promote 2D nucleation, despite the presence of phosphonate groups, which are expected to inhibit.^{21, 14} In addition, lattice matching as well as charge density criteria suggests that barium sulfate should also be inhibited by this phosphonated molecule. Yet this is not observed.

We hypothesise that the cause of this unusual behaviour is related to the ability of the BTP and BTS to de-hydrate the barium ion somewhat. This is a known kinetic energy barrier for barium sulfate crystallization.³⁰ If the binding of the cation to the organic anion is too strong, strong complexation and strong surface interaction can occur leading not only to a lowered cation activity but also to inhibition.²⁸ This is likely to be the case for calcium ions in the presence of BTP and BTS. If the binding of the organic anion to cation is relatively weak then this would aid crystallization, as noted previously.^{31, 32} This may be the case for barium ions. In addition, promotion followed by inhibition as the concentration of additive increases has been observed previously for calcium carbonate and barium sulfate.^{32, 33} We observe here results consistent with a strong interaction of the BTP and BTS with calcium ions and a weak interaction of the BTS and BTP with barium ions, thus resulting in promotion for barium sulfate but inhibition for calcium carbonate. While no data exists for the solution complexation behaviour of either BTS or BTP with calcium or barium ions, we have found the log K (complexation constant) values for phosphate complexed with calcium and barium ions³⁴ (1.87 and 1.36 respectively), showing the appropriate trend in support of this hypothesis. However, to clearly demonstrate that this is indeed the mechanism, we intend to undertake a molecular dynamics study, which would elucidate the kinetic energy barriers of the system and the impact of BTP and BTS on this.

Another possible contributor to this effect is the mode of adsorption of these molecules at growth features of the different inorganic species. That is, if the mode of adsorption alters for the two systems this may make crystallization more or less likely. However, infrared spectroscopy of phosphonates and sulfonates on barium sulfate is not trivial given the overlap of bands³⁵ thus in future work we will endeavour to ascertain from AFM experiments whether the adsorption mode (upright or flat) is a key parameter.

Conclusions

In conclusion, we have demonstrated for the first time, (as far as the authors are aware) of an organic molecule (BTP) that has a different mode of action on the crystallization of inorganic crystals. Furthermore, the presence of phosphonate groups on the organic molecule would be expected to show inhibitory effects on barium sulfate while experimentally, crystallization promotion is observed. The BTS and BTP molecules inhibit calcium carbonate crystallization while they

promote barium sulfate growth (and in the case of BTP, 2D nucleation also). This is significant for at least two reasons:

- i) Neither stereochemistry, nor charge density can explain why these molecules promote barium sulfate crystallization (meaning that 'lattice matching'¹⁴ or 'non-specific electrostatic interactions'³⁶ are not significant in this instance)
- ii) The possibility arises whereby one crystal system can be inhibited while another is promoted, thus opening up the potential for much greater control of crystallization systems with appropriately designed additives.

In addition, it is shown that while phosphonates are generally believed to be strong inhibitors they can also promote crystallization. Thus, functional group does not dictate impact on crystallization. In particular, the BTS molecule was shown to promote growth of barium sulfate within a specific concentration range, while inhibiting 2D and 3D nucleation. This resulted in no significant impact being observed on the barium sulfate de-supersaturation rate in batch experiments. On the other hand, the BTP molecule showed weaker 3D nucleation inhibition while 2D nucleation was promoted leading to a noticeable increase in the batch de-supersaturation rate.

We hypothesise that the different impacts of these organic molecules is related to the strength of interactions with the two cations; being a strong interaction with calcium ions and a relatively weak interaction with barium ions. These additives may also impact on the nearby water structure, which may or may not also be contributing to the different behaviours observed in this particular instance.^{37, 38} The strong interaction with calcium ions means a strong interaction with the surface leading to strong adsorption of the organic and to inhibition while the weaker interaction with barium ion leads to less adsorption at the surface but results in a partial de-hydration of the barium ion leading to promotion as observed for aspartic acid.³²

We have begun to study this behaviour computationally as further mechanistic understanding may be difficult to obtain experimentally.

Notes and references

*Nanochemistry Research Institute, Department of Chemistry, Curtin University, GPO Box U1987, Perth WA 6845 Australia.

‡ Corresponding author: Dr. F. Jones Phone: +618 9266 7677

Fax: +618 9266 4699 email: F.Jones@curtin.edu.au

^University of Calgary, Department of Chemistry
2500 University Drive NW, Calgary, Alberta, Canada T2N 1N4

† Electronic Supplementary Information (ESI) available: [details of any supplementary information available should be included here]. See DOI: 10.1039/b000000x/

1. K. S. Sorbie and E. J. Mackay, *J. Petroleum Sci. Eng.*, 2000, **27** 85.
2. W. J. Benton, I. R. Collins, I. M. Grimsey, G. M. Parkinson, and S. A. Rodger, *J. Chem. Soc. Faraday Disc.*, 1993, **95** 281.
3. P. J. Breen, H. H. Downs and B. N. Diel, *Spec. Publ. - R. Soc. Chem.*, 1991, **97** 186.
4. H.-C. Schwarzer and W. Peukert, *Chem. Eng. Technol.*, 2002, **25**(6) 657.
5. G. H. Nancollas, *Adv. Colloid Interface Sci.*, 1979, **10** 215.
6. Z. Amjad, *J. Colloid & Interface Sci.*, 1988, **123** 523.

7. H. H. Teng, P. M. Dove, C. A. Orme and J. J. de Yoreo, *Science*, 1998, **282**(5389) 724.
8. S. Mann (2001) in *Biomaterialization: Principles and Concepts in Bioinorganic Materials Chemistry* Oxford University Press, UK.
9. a) L.A. Gower and D. A. Tirrell, *J. Crystal Growth*, 1998, **191** 1. b) L. B. Gower and D. J. Odom, *J. Crystal Growth*, 2000, **210**(4) 719.
10. F. Jones, A. Oliveira, A. L. Rohl, M. I. Ogden, G. M. Parkinson, and M. M. Reyhani, *J. Crystal Growth*, 2002, **237-239** 424.
11. H. Cölfen, *Current Opinion in Colloid & Interface Sci.*, 2003, **8**(1) 23.
12. L. Qi, H. Cölfen and M. Antonietti, *Angew. Chemie Int. Ed.*, 2000, **39**(3) 604.
13. F. Jones, W. R. Richmond and A. L. Rohl, *J Phys Chem B*, 2006, **110** 7414.
14. S. N. Black, L. A. Bromley, D. Cottler, R. J. Davey, B. Dobbs and J. E. Rout, *J. Chem. Soc. Faraday Trans.*, 1991, **87**(20) 3409.
15. C. M. Pina, U. Becker, P. Risthaus, D. Bosbach, A. Putnis, *Nature*, 1998, **395**(6701) 483.
16. P. Risthaus, D. Bosbach, U. Becker, A. Putnis, *Colloids & Surfaces A*, 2001, **191** 201.
17. P. Fenter, M. T. McBride, G. Srajer, N. C. Sturchio, D. Bosbach, *J. Phys. Chem B*, 2001, **105**(34) 8112.
18. L. Addadi, Z. Berkovitch-Yellin, I. Weissbuch, M. Lahav and L. Leiserowitz, *Top. Stereochem.*, 1986, **16** 1.
19. F. Jones, M. Mocerino, M. I. Ogden, A. Oliveira and G. M. Parkinson, *Crystal Growth & Design*, 2005, **5**(6) 2336.
20. F. Jones, S. Piana and J. D. Gale, *Crystal Growth & Design*, 2008, **8**(3) 817.
21. K. Ichikawa, N. Shimomura, M. Yamada and N. Ohkubo, *Chem. Eur. J.*, 2003, **9** 3235.
22. F. Jones, J. Clegg, A. Oliveira, A. L. Rohl, M. I. Ogden, G. M. Parkinson, A. M. Fogg and M. M. Reyhani, *CrystEngComm*, 2001, **3**(40) 165.
23. S. R. Freeman, F. Jones, M. I. Ogden, A. Oliviera and W. R. Richmond, *Crystal Growth & Design*, 2006, **6**(11) 2579.
24. F. Jones, P. Jones, M. I. Ogden, W. R. Richmond, A. L. Rohl and M. Saunders, *J. Colloid & Int. Sci.*, 2007, **316** 533.
25. S. Shinkai, K. Araki, T. Tsubaki, T. Arimura and O. Manabe, *J. Chem. Soc. - Perkins Trans.*, 1987, **1**(11) 2297.
26. B. D. Chandler, G. D. Enright, K. A. Udachin, S. Pawsey, J. A. Ripmeester, D. T. Cramb and G. K. H. Shimizu, *Nature-Mater.*, 2008, **7** 229.
27. K. C. Yang and R. Hogg, *Analytical Chemistry*, 1979, **51**(6) 758.
28. J. W. Mullin (1961), *Nucleation*. In *Crystallization*, 3rd ed.; Butterworth-Heinemann: Oxford, pp 172-201.
29. T. F. Kazmierczak, M. B. Tomson and G. H. Nancollas *J. Phys. Chem.*, 1982, **86** 103.
30. P. M. Schindler and W. Stumm, "Aquatic surface chemistry" ed W. Stumm, Wiley, New York 1987, 83-110.
31. S. Piana, F. Jones and J. D. Gale, *J. Am. Chem. Soc.*, 2006, **128**(41) 13568.
32. S. Piana, F. Jones and J. D. Gale, *CrystEngComm*, 2007, **9** 1187.
33. S. Elhadj, J. J. De Yoreo, J. R. Hoyer and P. M. Dove, *PNAS*, 2006, **103**(51) 19239.
34. P. May, K. Murray, "Joint Expert Speciation System", an online thermochemical database for modelling aqueous solution chemistry, containing speciation and complexation data. http://jess.murdoch.edu.au/jess/jess_home.htm
35. F. Jones, P. Jones, R. De Marco, B. Pejic and A. L. Rohl, *Applied Surface Science*, 2008, **254**(11) 3459.
36. (a) D. Volkmer, M. Fricke, C. Agena and J. Mattay, *J. Materials Chemistry*, 2004, **14** 2249. (b) D. Volkmer, M. Fricke, C. Agena and J. Mattay, *CrystEngComm*, 2002, **4**(52), 288. (c) M. Fricke, D. Volkmer, C. E. Krill III, M. Kellermann and A. Hirsch, *Crystal Growth & Design*, 2006, **6**(5), 1120.
37. S. D. Škapin, I. Sondi, *J. Colloid and Interface Sci.*, 2010, **347**(2), 221.
38. M. Kowacz, C. V. Putnis, A. Putnis, (2007), *Geochim. et Cosmochim. Acta.*, **71** 5168. (b) M. Kowacz, A. Puntis (2008), *Geochim. et Cosmochim. Acta* **72** 4476. (c) M. Kowacz, M. Prieto, A. Putnis (2010), *Geochimica et Cosmochimica Acta*, **74**(2) 469.